Enhancing cell packing in buckyballs by acoustofluidic activation

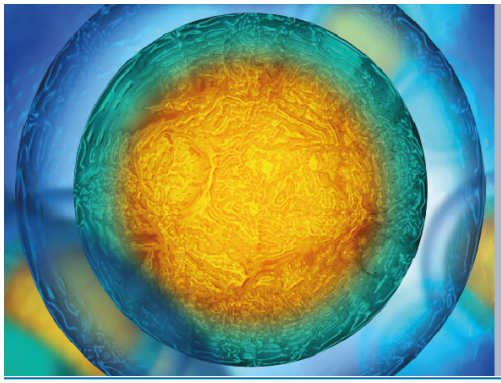

Biofabrication

PAPER

Enhancing cell packing in buckyballs by acoustofluidic activation

Tanchen Ren[1], Wolfgang Steiger[2,3], Pu Chen[4,5], Aleksandr Ovsianikov[2,3,6] and Utkan Demirci[1,6]

[1] Bio-Acoustic MEMS in Medicine (BAMM) Laboratory, Canary Center at Stanford for Cancer Early Detection, Department of Radiology, Stanford School of Medicine, Palo Alto, California 94304, United States of America
[2] Institute of Materials Science and Technology, TU Wien, Getreidemarkt 9, 1060 Vienna, Austria
[3] Austrian Cluster for Tissue Regeneration (http://tissue-regeneration.at), Vienna, Austria
[4] Department of Biomedical Engineering, Wuhan University School of Basic Medical Sciences, Wuhan 430071, People's Republic of China
[5] Hubei Province Key Laboratory of Allergy and Immunology, Wuhan, Hubei 430071, People's Republic of China
[6] Authors to whom any correspondence should be addressed.

E-mail: aleksandr.ovsianikov@tuwien.ac.at **and** utkan@stanford.edu

OPEN ACCESS

RECEIVED
25 August 2019

REVISED
1 January 2020

ACCEPTED FOR PUBLICATION
17 February 2020

PUBLISHED
31 March 2020

Keywords: packing, cell aggregation, buckminsterfullerene, two-photon printing, neuronal network

Supplementary material for this article is available online

Abstract

How to pack materials into well-defined volumes efficiently has been a longstanding question of interest to physicists, material scientists, and mathematicians as these materials have broad applications ranging from shipping goods in commerce to seeds in agriculture and to spheroids in tissue engineering. How many marbles or gumball candies can you pack into a jar? Although these seem to be idle questions they have been studied for centuries and have recently become of greater interest with their broadening applications in science and medicine. Here, we study a similar problem where we try to pack cells into a spherical porous buckyball structure. The experimental limitations are short of the theoretical maximum packing density due to the microscale of the structures that the cells are being packed into. We show that we can pack more cells into a confined micro-structure (buckyball cage) by employing acoustofluidic activation and their hydrodynamic effect at the bottom of a liquid-carrier chamber compared to randomly dropping cells onto these buckyballs by gravity. Although, in essence, cells would be expected to achieve a higher maximum volume fraction than marbles in a jar, given that they can squeeze and reshape and reorient their structure, the packing density of cells into the spherical buckyball cages are far from this theoretical limit. This is mainly dictated by the experimental limitations of cells washing away as well as being loaded into the chamber.

1. Introduction

Physics and mathematics define fundamental problems in biology and bioengineering [1]. For instance, the particle packing problem can be a simplified model for cell aggregation and spheroid formation. How many cells can be packed into a confined space is similar to the question of how many gumball candies can be packed into a jar? The sphere packing model has been experimentally and theoretically studied for centuries and has recently evolved with the realization that particle shapes, materials, and packing tightness all change the packing volume fraction, ϕ, which is defined as the percentage of space occupied by the packed particles [2]. To apply this theory in cell packing, there are certain challenges such as the deformability that must be considered since cells are soft objects. Only a few studies have reported packing using soft materials such as polyelectrolyte gels to study the contact force of packing [3]. Theoretically studying the lattice packing of soft particles has also been reported as a model for protein packing in molecular biology [4]. Further, cell aggregation still remains as an interesting subject in soft material packing, which is important for cell packing in 3D biomaterial scaffolds and cell delivery tissue engineering.

Creating cellular aggregates with the highest density of packing is achieved by free-form assembly of cellular spheroids [5] using various methods such as the hanging drop [6], low-adhesion culture plate [7], PDMS templates [8], microfluidic [9, 10], magnetic

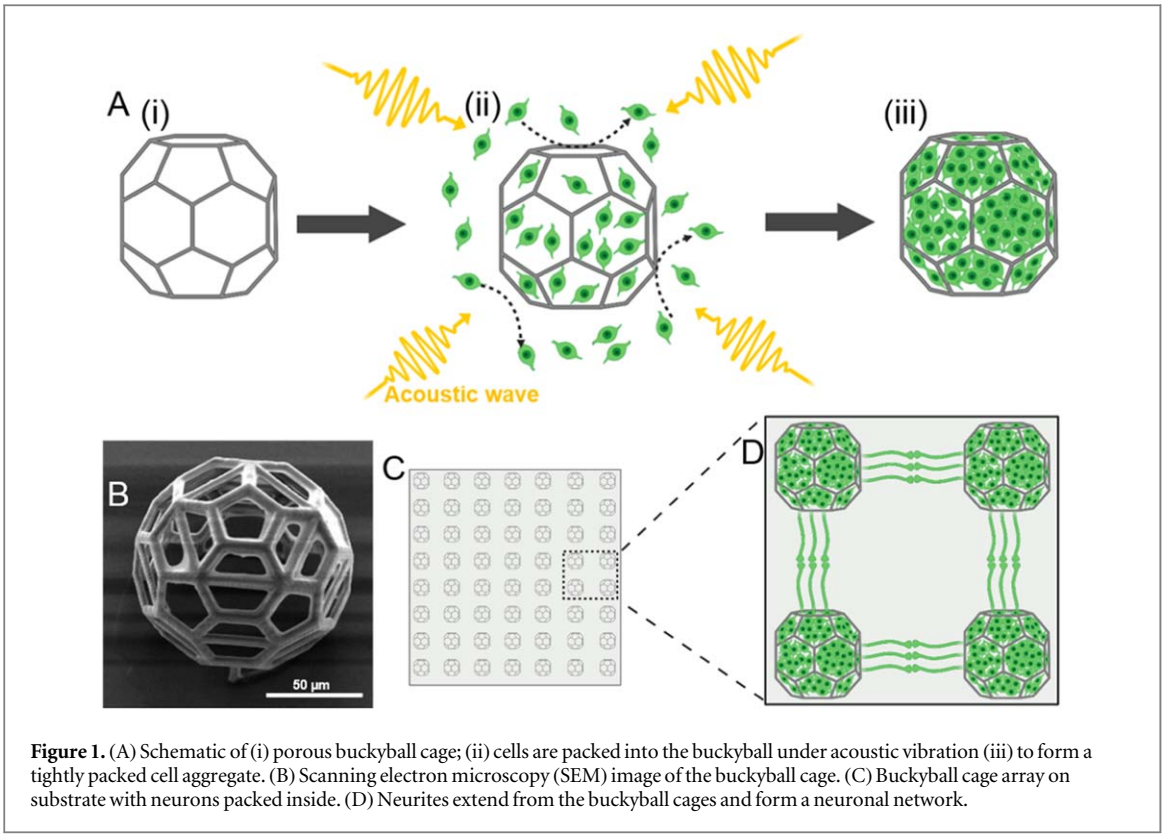

Figure 1. (A) Schematic of (i) porous buckyball cage; (ii) cells are packed into the buckyball under acoustic vibration (iii) to form a tightly packed cell aggregate. (B) Scanning electron microscopy (SEM) image of the buckyball cage. (C) Buckyball cage array on substrate with neurons packed inside. (D) Neurites extend from the buckyball cages and form a neuronal network.

[11], and acoustic assembly [12]. How cells pack in a porous cage scaffold can also be an interesting strategy as cell aggregate distribution can be predefined by cage design. When a scaffold is used for cell packing, another question arises: How many cells can enter and stay in that scaffold? This can be simplified as a question about random number distributions as cells will distribute randomly onto the substrate. There are two ways to increase cell packing efficiency in scaffolds, one is to increase the number of cells entering the cavities of a scaffold and the other is to reduce the cells escaping from the scaffold. The ability of cells to escape is mainly determined by the ratio between the cell and pore size, which can be considered as an intrinsic property. There are several ways to motivate cells to enter scaffold cavities and increase cell packing, for instance, capillary force and vacuum can accelerate cell loading to scaffold cavities. However, these methods are not functional when the scaffold is already wet in a liquid phase.

In this paper, we present an acoustic assisted packing strategy which can locomote cells in liquid by acoustofluidic activation and their hydrodynamic effect at the bottom of a liquid-carrier chamber. This enables loading of wet scaffolds with cells in suspension. We designed buckyball microcages inspired by the shape of the buckminsterfullerene (C60) molecule [13] to use as microscale porous base units for cell packing. The acoustofluidic-induced hydrodynamic pressure can increase cell loading into the microscale buckyball cages (figures 1(A) and (B)). By packing neurons into an array of buckyballs (figure 1(C)), we form a network of neurite extensions (figure 1(D)).

2. Experimental methods

2.1. Buckyball cage fabrication

A two-photon laser printing system (2PL; MaiTai, DeepSee, Newport/Spectra Physics, Santa Clara, USA) was used to print the buckyball as previously described [14]. Zr-Hybrid (SZ2080) with 0.1 wt% 4,4′-Bis (diethylamino)benzophenone (Merck KGaA, Darmstadt, Germany) was dissolved in 1-propanol and allow to dried before 2PP (two-photon polymerization) processing using a heating plate set to 40 °C for 2–3 h. The fabrication was done with a laser power of 70 mW, at a fabrication speed of 40 mm s^{-1}. The hatching spacing was $\Delta h = 0.2$ μm and the layer distance was $\Delta z = 0.5$ μm. Alternating x- and y-scanning directions for subsequent layers were used to obtain the 3D structures. The diameter of the buckyballs was 100 μm, with a pore size of ≈32 μm for the pentagon area and ≈40 μm for the hexagon area (figures 1(B) and S1(A) (figure S1A is available online at stacks.iop.org/BF/12/025033/mmedia)). To decrease the pore size a central rod was added to the hexagon area. A 63 × /1.4 oil immersion objective was chosen for the 2PL printing system due to the requirement of high resolution [15]. The operating wavelength of the laser was 800 nm. On a 9 × 9 mm cover slide, an array of a 25 × 25 buckyball connected to the glass was 3D bioprinted. The space between each buckyball is 240 μm in both the x- and y-directions

(figure S1(B)). The structure can be safely preserved in the dark for years before any cell experiments. To expose the buckyballs, the samples were submerged in 1-propanol and developed for at least 1 h to remove the unpolymerized materials. After washing in propanol several times, clean buckyball cages were dried in a sterile environment before use.

To study the effect of geometry on the trapping efficiency, three buckyball designs were compared: complete ('o'-shaped), open top ('u'-shaped), and open bottom buckyball ('n'-shaped) (figure 3). The size and distribution of the buckyballs were consistent with the previous experiment as shown in figure 1(B).

2.2. SEM of Buckyball cages

Samples were sputtered with gold for 30 s before SEM imaging. SEM was operated at U = 15 kV under a pressure $<10^{-5}$ mbar. Images were recorded using 4× averages and integrating the image acquisition.

2.3. Cell culture

NIH 3T3 murine fibroblasts were cultured in Dulbecco's modified Eagle's medium supplemented with 10% fetal bovine serum and 1% penicillin/streptomycin. Human umbilical vein endothelial cells (HUVECs) were cultured in EGM-2 (Lonza). Primary cortical neurons were isolated from embryonic day 18 (E18) CD-1 mice were provided by Charles River as described previously [16, 17]. All experiments were carried out according to animal care standards set forth by the National Institutes of Health and were approved by the Institutional Animal Care and Use Committee at Stanford University. Freshly microdissected whole mouse cortices were dissociated by trituration after 30 min of enzymatic digestion using Neuronal Isolation Enzyme (Thermo Scientific) in Hanks' balanced salt solution without Mg^{2+} and Ca^{2+} (HBSS(-), Life Technologies). The neurons were then suspended in a neurobasal medium with B27 supplement (Life Technologies) and 500 μM of glutamine (Life Technologies). Culture conditions were maintained at 37 °C with a 95% relative humidity and 5% CO_2. Substrates with buckyball cages were coated with poly-D-lysine (PDL; 100 μg ml^{-1}, Sigma) for 1 h and washed twice with ddH_2O before being loaded with cortical neurons.

2.3.1. Acoustofluidic activation

To generate the acoustic acoustofluidic activation, a waveform generator (33500B Series, Agilent) was used to generate sinusoidal waves with a frequency of 54 Hz and an amplitude of 80 mVpp which was then amplify by a power amplifier (Lepai LP-2020Aþ, Parts Express) before being transferred to a vibration generator [18]. A square-shaped liquid container (10 × 10 × 1 mm) was mounted on top of the vertical vibration (U56001, 3B Scientific). After putting the glass slide with buckyballs at the bottom of the container, 100 μl of cell culture medium with 2 M ml^{-1} of cells were added. After vibrating for 100 or 300 s, the glass slides were carefully removed from the cell suspension, dipped in fresh medium slowly once and then transferred to a 12 well plate with 1 ml of culture medium. Because of the small size of the buckyball and surface tension of liquid, the structures could hold the medium inside to avoid the cells from being washed away. Buckyball slides were put inside the chamber without vibration, where the cells that settled under gravity were set as controls. The experimental results were collected from $n = 3$ buckyball substrates. For 3T3 and HUVEC, the cells were only cultured for 24 h, and the medium was not changed during the culture; for the cortical neurons, the cells were cultured for 7 days and 50% of the medium was changed at days *in vitro* (DIV) 3 and DIV 5.

2.4. Cell staining and imaging

NIH 3T3 cells were labeled with cell nuclei dye Hoechst 33342 (blue) and Cytoplasma dye CellTrace™ Far Red (Cy5) before counting. Bright field and fluorescence images were taken using a Zeiss AxioObserver Z1 microscope at 5× and 20× magnifications.

The primary cortical neurons were cultured for 7 days before being fixed with 4% paraformaldehyde (Electron Microscopy Sciences) in PBS for 30 min at room temperature. Following being washed 3× with PBS, 3D tissues were permeabilized in PBS containing 0.25% Triton X-100 (Sigma-Aldrich) for 3 min at room temperature, and then incubated in 1% (w/v) bovine serum albumin (Sigma-Aldrich) in PBS for 1 h at 37 °C. The cells were stained with 1:300 rabbit anti-β-tubulin (Tuj1, Abcam, ab18207) followed by secondary antibody Alexa Fluor 568 donkey anti-rabbit (1:500, red, Jackson ImmunoResearch Laboratory) staining for 1 h. After being washed with PBS, 4′,6-Diamidino-2-phenylindole, dihydrochloride (1:1000, Life Technologies) was added into the staining solution for nuclear staining. Fluorescence images were taken using a Zeiss AxioObserver Z1 microscope at 10× magnification.

The cell numbers were counted using the ImageJ software (NIH) based on the nuclear numbers inside each cages. An ImageJ screenshot is shown in figure S3 to demonstrate how the cell numbers were counted. The total neurite length was quantified by an ImageJ plugin, NeuphologyJ, which could automatically trace the outgrowing neurites in the whole image.

3. Results

On all the substrates with o-type buckyball cages, the cells were mainly located inside the buckyballs since the free cells were washed away during the rinsing steps. The cell packing was improved by acoustic vibrations. In the control group without acoustic vibrations, 37% of the buckyball cages were empty;

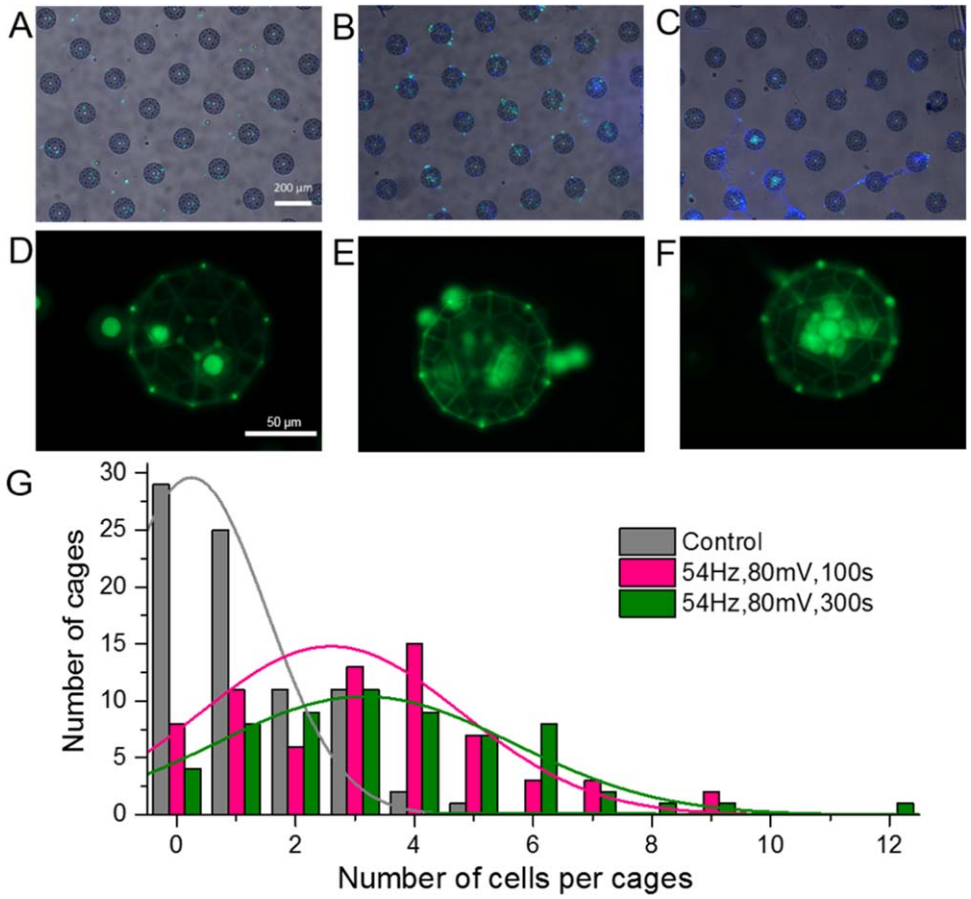

Figure 2. NIH 3T3 fibroblast stained with Hoechst 33342 (nuclear, blue) and CellTrace CSFE (cytoplasma, green) were packed into a buckyball cage array under acoustic vibration. (A)–(C) Merged image of fluorescence channels and bright field channels of cell loading on the buckyball array. (D)–(F) 20× fluorescence image showing the cell packing in buckyball cages. (A), (D) without acoustic vibration (control), (B), (E) after 100 s acoustic vibration, and (C), (F) after 300 s acoustic vibration. (G) Distribution of cages based on the cell packing numbers inside the buckyball.

Table 1. Statistical results of the number of cages and cells studied and the average cell packing number in the o-shaped buckyball cages under different acoustic vibration times: 0, 100, and 300 s.

Statistics	Total number of cages	Total number of cells	Average number of cells	Standard deviation
Control	79	93	1.2	1.2
54 Hz, 80 mV, 100 s	68	214	3.1	2.2
54 Hz, 80 mV, 300 s	61	221	3.6	2.4

32% of the cages had only one cell, and 14% of the cages had two cells inside (figures 2(D), (G)). When we introduce acoustic vibrations for 100 s, we observed a significant increase in cell capture inside the cages (figures 2(B), (E), and (G)). Under the acoustofluidic activation, the average number of captured cells increased from 1.2 ± 1.2 to 3.1 ± 2.2 (table 1). And the cages comprising four cells had the highest percentage (23%) among all the buckyball cages on the substrate. However, prolonging the vibration time to 300 s did not increase the cell packing efficiency, with similar average cell numbers of 3.6 ± 2.4 cells in each cage, where 21% of the buckyball cages were loaded with three cells which is the highest percentage among all of the buckyball cages. For each single buckyball cage, the number of cells being trapped inside could be of large variation when the cell density in the bulk environment was low. The natural process of cell trapping inside the buckyball cages is a completely random distribution which follows a Gaussian distribution. The right shift of the Gaussian distribution curves (curve center shifted from 0.6 to 3.0+) after acoustic treatment, indicated cell packing enhancement. The standard deviations (σ) of the fitting curves with or without acoustic activation are similar, although they were large, they agreed with the random distribution. To test whether increasing the cell number in a liquid environment can enhance cell packing, a 4 M ml^{-1} cell suspension was used to pack HUVECs in the buckyballs (figure 3). An average of 10.9 ± 2.2 cells were located inside the cages after acoustic vibration. Increasing the cell packing number

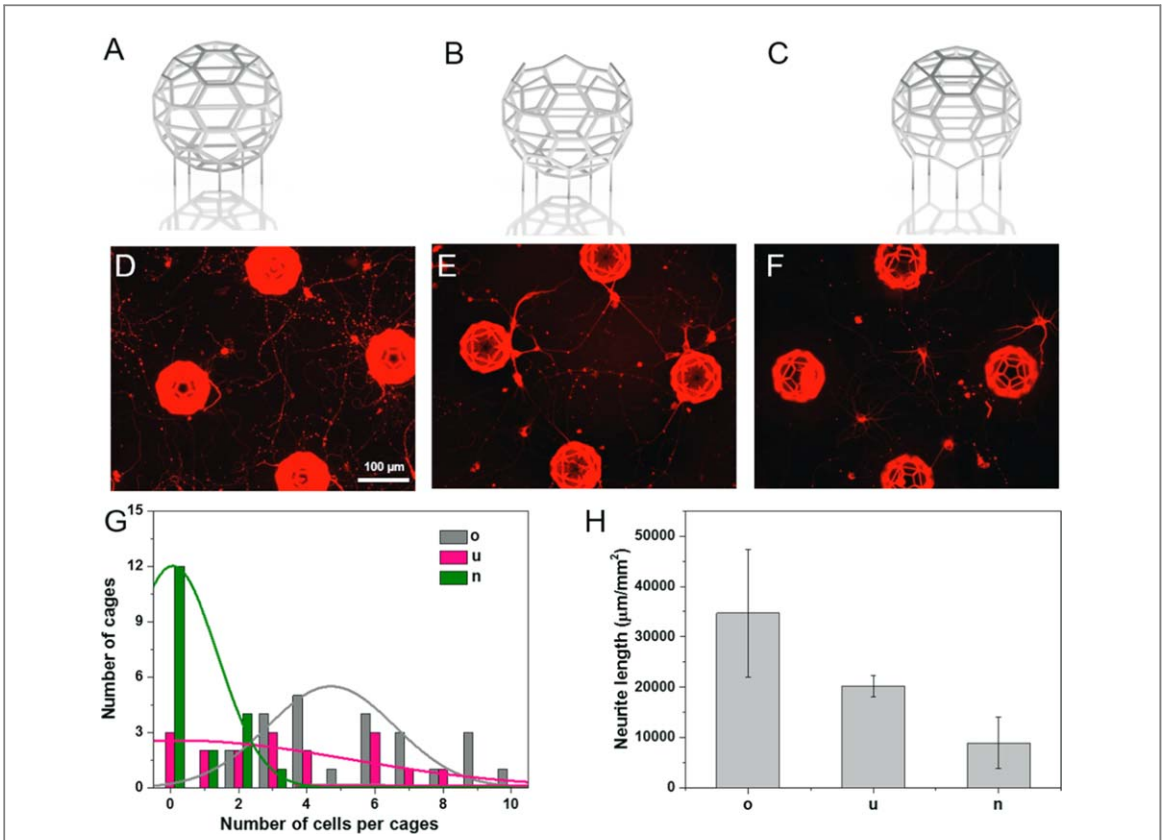

Figure 3. The primary cortical neurons were packed into buckyball cage arrays with different openings under acoustic vibration. (A)–(C) Schematic design of (A) complete (o-shaped), (B) open top (u-shaped), and (C) open bottom (n-shaped) buckyballs. The size and distribution of the buckyballs were consistent with figure 1(B). (D)–(F) Fluorescence image showing the neuronal network stained with anti β-tubulin (red) at day 7 of culture after acoustic cell packing of the buckyball cage array. (A), (D) o-shaped cages (B), (E) u-shaped cages, and (C), (F) n-shaped cages. (G) Distribution of cages based on the cell packing numbers inside the buckyball. (H) Statistical results of the total neurite length on the substrate of the buckyball array at D7.

Table 2. Statistical results of the number of cages and cells studied and the average cell packing number in the o-shaped, u-shaped, and n-shaped buckyball cages.

Statistics	Total number of cages	Total number of cells	Average number of cells	Standard deviation
u	17	56	6.2	2.6
n	19	13	1.3	6.0
o	24	131	10.5	2.5

also reduced the relative value of the deviation in the cell packing when the absolute value was still $\sim\pm 2$.

As prolonging the acoustic vibration duration does not increase packing density, we designed different geometries for buckyballs as models to evaluate the number of cells entering and staying in the cages. The three models are the full sphere (we define as o-shaped, figure 3(A)), open bottom (n-shaped, figure 3(B)), and open top (u-shaped, figure 3(C)). Here, we used primary cortical neurons for the cell packing experiments. The average cell packing number was 6.2 ± 2.6 cells in the u-shaped cages, and 1.3 ± 1.0 cells in the n-shaped cages, while 10.5 ± 2.5 cells were found in the o-shaped cages (table 2). For the cell number distribution, all of the o-shaped cages were loaded with cells, and 4% of the cages had as many as 10 cells packed inside. The u-shaped cages had a nearly equal distribution for packing 0–6 cells. We observed that 63% of the n-shaped cages had no cells inside (figure 3(D)). We concluded that cells could be more easily washed away when there was an opening on the cage. The bottom opening led to more cells being washed away as compared to the top opening. We hypothesize that in the n-shaped structures, cells may fall out from the buckyball cages easier at a static state. In the u-shaped cages, although there is a higher possibility of cells escaping during the rinsing, most of the cells could be preserved thanks to the short rinsing time and the surface tension of the liquid. We also used a positive chemical modification by poly-D-lysine (PDL) to increase the overall neuronal cell affinity of the substrate. We observed a higher cell packing number in the o-shaped cages with surface modification compared to the earlier experiments using 3T3 cells without surface modification. In the neuron loaded cages, neurites extended out from the porous cages and formed connected networks in the o-shaped and u-shaped cages. The neurite length was 35 mm mm^{-2} on the substrate with the o-shaped buckyball array, 20 mm mm^{-2} on the u-shaped buckyball array, and 9 mm mm^{-2} on the n-shaped

cage arrays. In the n-shaped cages, the packing was low and the number of neurons was too low to support healthy neuron growth as cell density also plays an important role in neuronal growth [19], so the neurite length was significantly shorter on the substrates with n-shaped cages.

4. Discussion

Efficient packing is definitely a significant question both theoretically and experimentally. We came to realize the fact that at the scale that we were operating at, the major limitations were more on the inability to force the cells into a specific location at the microscale in a high throughput manner. Theoretically, we hypothesize that cell packing can reach the highest volume fraction packing of spheres as the cells in suspension can be considered a sphere shape. Thus, $\phi = 0.74$, which means 74% of the volume will be occupied by cell spheres. The inner volume of the buckyball cage is $\sim 5.2 \times 10^5\ \mu m^3$, and the volume of the cells is $\sim 5.2 \times 10^2\ \mu m^3$ as we take the cell diameter to be around 10 μm. As a result, 740 cells can be packed inside the buckyball cage in theory. This does not consider the deformation of cells which will further increase the volume fraction. Compared to previous research using acoustic waves for cell assembly, where an $\sim 0.3 \times 10^9$ cell ml^{-1} density was reached (means 156 cells were packed in the volume of the buckyball cage) [20], the packing density in the buckyball was also much lower because the cage boundary hindered part of cells entering the cage and part of the cells escaped during the washing process.

Some solutions for this have been proposed such as using magnetic fields with microparticles [21], iron oxide nanoparticles to assemble cells [22], or particle free magnetic levitation approaches [11, 22–24] and surface chemistry immobilization [25] and acoustic assembly within a droplet [26] and acoustic waves to assemble cells at a larger scale [18, 20, 27]. All these approaches mainly focus on the assembly of cells to cells without any predefined configuration, where here we presented moving cells with a field to pack them in a spherical buckyball using acoustic vibrations. Optical traps [28] could potentially also be a method to command over a single cell to move it into a buckyball. However, these approaches are slow given the number of balls that need to be filled and the limitation around having a single laser beam and its associated costs for time and equipment.

The fused-ring structure of a buckyball is highly stable to high pressure [29], while offering a large opening on the surface for cells to enter. As a result, the buckyball structure is a great candidate for a microscale cell packing study. We used a buckyball as a proof-of-concept for acoustic accelerated cell packing, which can also act as a base to predict cell packing for other shapes as they can be considered as the combination of multiple buckyball. The shape and the open porosity of the microscale buckyballs allows cell–cell communication between neighboring cages to form integrated structures. For example, the ideal cell packing number of a dumbbell-shaped cage formed as shown in figure S5 can be calculated by summing the cell numbers in two individual buckyballs. For cages with a larger size and different geometries, it is important to make sure there are no large openings for cells to escape from.

While there are limitations in the packing density of cells trapped within buckyballs, the advantage of a buckyball array is to control the cell seeding location. The buckyball array determines the location where the cells adhered since cells at all the other locations were washed away.

For cells with proliferation ability, although the cell packing number cannot reach a dense packing initially to fully fill the buckyballs, cell division can lead to the formation of densely packed microcages. In figures S3(B) and (D), 7% of the microcages reached dense packing in 24 h of culture. The formed 3D cellular structures are highly consistent in size and morphology, due to the precisely controlled geometry of the buckyballs. This can help to create predesigned cellular structures by tuning the manner in which buckyballs connect (i.e. adding a bridge between two buckyball cages, figure S5) or distributing the density to form different 3D cellular networks. The 3D cellular structures are shielded by the buckyball cage from mechanical damage during handling. Besides, the design of a 3D cellular structure can also be across time and space using 2PP buckyball cages. Before removing the unpolymerized materials, the printed buckyballs can be preserved in the dark for months or even years and shipped between different locations. These can benefit multi-institute collaborations for 3D organ-on-a-chip studies and applications when used as a platform technique.

5. Conclusions

We show that the acoustic field performs better in packing cells into a confined cage compared to just random filling of cells. However, given the theoretical filling densities, we need to address the main limitations in achieving high packing densities of cells into buckyballs, which arise from the fact that we do not have the necessary high throughput microscale tools to fill multiple micro-chambers precisely like filling jars with multiple marbles at a time. Although the packing density is significantly lower than ideal tight packing, a neuronal network was still formed on the buckyball array through sending extensions to neighboring cages. Although packing density is far from ideal packing, we believe that an acoustic field can become a potential solution for increasing packing

density in a defined micro-structure for tissue engineering.

Acknowledgments

The authors would like to acknowledge the financial support by the Canary Foundation Awards the European Research Council (Consolidator Grant-772464), the FWF-FWO grant (Austrian Science Fund project #I2444N28), and Applied Foundational Research Program of Wuhan Municipal Science and Technology Bureau (No. 2018010401011296). The authors would like to thank Prof. Vladimir Mironov, professor at Ivanovo Sate Medical University in Russia, for useful discussions; Mehmet Giray Ogut, a visiting undergraduate student at the Canary Center at Stanford University, for the assistance with the drawing of the schematic figures; and Hojae Lee, a research technician at the Canary Center at Stanford University for support on the experiments. The authors would like to thank Sihan Chen, Nian Liu, and Jibo Wang in the Department of Biomedical Engineering, Wuhan University School of Basic Medical Sciences for their assistance in the theoretical evaluation of acoustofluidic activation.

ORCID iDs

Tanchen Ren https://orcid.org/ 0000-0002-3382-7042
Pu Chen https://orcid.org/0000-0002-6857-2211
Aleksandr Ovsianikov https://orcid.org/0000-0001-5846-0198
Utkan Demirci https://orcid.org/0000-0003-2784-1590

References

[1] Beebe D J, Mensing G A and Walker G M 2002 Physics and applications of microfluidics in biology *Annu. Rev. Biomed. Eng.* **4** 261–86
[2] Weitz D A 2004 Packing in the spheres *Science* **303** 968
[3] Lachhab T and Weill C 1999 Compression of a soft sphere packing *Eur. Phys. J.* B **9** 59–69
[4] Edelsbrunner H and Iglesias-Ham M 2018 On the optimality of the FCC lattice for soft sphere packing *SIAM J. Discrete Math.* **32** 750–82
[5] Ovsianikov A, Khademhosseini A and Mironov V 2018 The synergy of scaffold-based and scaffold-free tissue engineering strategies *Trends Biotechnol.* **36** 348–57
[6] Foty R 2011 A simple hanging drop cell culture protocol for generation of 3D spheroids *J. Vis. Exp.* **51** 2720
[7] Maritan S M, Lian E Y and Mulligan L M 2017 An efficient and flexible cell aggregation method for 3D spheroid production *J. Vis. Exp.* 55544
[8] Gu Q, Tomaskovic-Crook E, Lozano R, Chen Y, Kapsa R M, Zhou Q, Wallace G G and Crook J M 2016 Functional 3D neural mini-tissues from printed gel-based bioink and human neural stem cells *Adv. Healthcare Mater.* **5** 1429–38
[9] Zuchowska A, Jastrzebska E, Chudy M, Dybko A and Brzozka Z 2017 3D lung spheroid cultures for evaluation of photodynamic therapy (PDT) procedures in microfluidic lab-on-a-chip system *Anal. Chim. Acta* **990** 110–20
[10] Li Y, Zhang T, Pang Y, Li L, Chen Z N and Sun W 2019 3D bioprinting of hepatoma cells and application with microfluidics for pharmacodynamic test of metuzumab *Biofabrication* **11** 034102
[11] Tocchio A, Durmus N G, Sridhar K, Mani V, Coskun B, El Assal R and Demirci U 2018 Magnetically guided self-assembly and coding of 3D living architectures *Adv. Mater.* **30** 1705034
[12] Wu Y, Ao Z, Bin C, Muhsen M, Bondesson M, Lu X and Guo F 2018 Acoustic assembly of cell spheroids in disposable capillaries *Nanotechnology* **29** 504006
[13] Kroto H W, Heath J R, O'Brien S C, Curl R F and Smalley R E 1985 C60: buckminsterfullerene *Nature* **318** 162–3
[14] Silva K R *et al* 2016 Delivery of human adipose stem cells spheroids into lockyballs *PLoS One* **11** e0166073
[15] Steiger W, Gruber P, Theiner D, Dobos A, Lunzer M, Van Hoorick J, Van Vlierberghe S, Liska R and Ovsianikov A 2019 Fully automated z-scan setup based on a tunable fs-oscillator *Opt. Mater. Express* **9** 3567–81
[16] Canadas R F, Ren T, Tocchio A, Marques A P, Oliveira J M, Reis R L and Demirci U 2018 Tunable anisotropic networks for 3D oriented neural tissue models *Biomaterials* **181** 402–14
[17] Ren T, Goldberg J L and Steketee M B 2018 *Regulating Growth Cone Motility and Axon Growth by Manipulating Targeted Superparamagnetic Nanoparticles* ed F Santamaria and X G Peralta (New York: Springer) pp 89–108
[18] Ren T, Chen P, Gu L, Ogut M G and Demirci U 2019 Soft ring-shaped cellu-robots with simultaneous locomotion in batches *Adv. Mater.* **32** 1905713
[19] Hartikka J and Hefti F 1988 Development of septal cholinergic neurons in culture: plating density and glial cells modulate effects of NGF on survival, fiber growth, and expression of transmitter-specific enzymes *J. Neurosci.* **8** 2967–85
[20] Serpooshan V *et al* 2017 Bioacoustic-enabled patterning of human iPSC-derived cardiomyocytes into 3D cardiac tissue *Biomaterials* **131** 47–57
[21] Xu F, Wu C A, Rengarajan V, Finley T D, Keles H O, Sung Y, Li B, Gurkan U A and Demirci U 2011 Three-dimensional magnetic assembly of microscale hydrogels *Adv. Mater.* **23** 4254–60
[22] Souza G R *et al* 2010 Three-dimensional tissue culture based on magnetic cell levitation *Nat. Nanotechnol.* **5** 291–6
[23] Subramaniam A B, Yang D, Yu H-D, Nemiroski A, Tricard S, Ellerbee A K, Soh S and Whitesides G M 2014 Noncontact orientation of objects in three-dimensional space using magnetic levitation *Proc. Natl Acad. Sci.* **111** 12980
[24] Berry M V and Geim A K 2017 Of flying frogs and levitrons *A Half-Century of Physical Asymptotics and Other Diversions* (Singapore: World Scientific) pp 615–21
[25] Cheng X, Irimia D, Dixon M, Sekine K, Demirci U, Zamir L, Tompkins R G, Rodriguez W and Toner M 2007 A microfluidic device for practical label-free CD4(+) T cell counting of HIV-infected subjects *Lab Chip* **7** 170–8
[26] Xu F, Finley T D, Turkaydin M, Sung Y, Gurkan U A, Yavuz A S, Guldiken R O and Demirci U 2011 The assembly of cell-encapsulating microscale hydrogels using acoustic waves *Biomaterials* **32** 7847–55
[27] Chen P, Guven S, Usta O B, Yarmush M L and Demirci U 2015 Biotunable acoustic node assembly of organoids *Adv. Healthcare Mater* **4** 1937–43
[28] Kreysing M, Ott D, Schmidberger M J, Otto O, Schurmann M, Martin-Badosa E, Whyte G and Guck J 2014 Dynamic operation of optical fibres beyond the single-mode regime facilitates the orientation of biological cells *Nat. Commun.* **5** 5481
[29] Kozlov M E, Tokumoto M and Yakushi K 1997 Spectroscopic characterization of pressure modified C60 *Appl. Phys.* A **64** 241–5